# Quantum criticality of the kagome antiferromagnet with Dzyaloshinskii-Moriya interactions

Yejin Huh,[1] Lars Fritz,[1,2] and Subir Sachdev[1]
[1]*Department of Physics, Harvard University, Cambridge, Massachusetts 02138, USA*
[2]*Institut für Theoretische Physik, Universität zu Köln, Zülpicher Straße 77, 50937 Köln, Germany*
(Received 10 March 2010; published 30 April 2010)

We investigate the zero-temperature phase diagram of the nearest-neighbor kagome antiferromagnet in the presence of Dzyaloshinksii-Moriya interaction. We develop a theory for the transition between $Z_2$ spin liquids with bosonic spinons and a phase with antiferromagnetic long-range order. Connections to recent numerical studies and experiments are discussed.

DOI: 10.1103/PhysRevB.81.144432 PACS number(s): 75.30.Kz, 75.10.Kt, 75.50.Ee

## I. INTRODUCTION

The nearest-neighbor spin $S=\frac{1}{2}$ antiferromagnet on the kagome lattice has been the focus of extensive theoretical and experimental studies because it is a prime candidate for realizing a ground state without antiferromagnetic order.

On the experimental side, much attention has focused on the $S=1/2$ compound herbertsmithite $ZnCu_3(OH)_6Cl_2$. It has $J\approx 170$ K and no observed ordering or structural distortion.[1–4] However, there is an appreciable amount of substitutional disorder between the Zn and Cu sites (believed to be of the order 5–10 %) which affects the low-$T$ behavior.[5–11] More importantly, there is an upturn in the susceptibility at $T=75$ K which has been ascribed to the Dzyaloshinksii-Moriya (DM) interactions.[5,12–15]

On the theoretical side, the most recent evidence[16–21] on the nearest-neighbor antiferromagnet points consistently to a ground state with a spin gap of $0.05J$ and valence-bond solid (VBS) order. The pattern of the VBS order is quite complex with a large unit cell, but was anticipated by Marston and Zeng[22] by an application of the VBS selection mechanism described in the $1/N$ expansion of the SU($N$) antiferromagnet.[23]

The influence of the DM interactions has also been studied theoretically.[15,24–26] Starting with an "algebraic spin-liquid" ground state, Hermele *et al.*[26] argued that the DM coupling, $D$, was a relevant perturbation, implying that an infinitesimal $D$ would induce long-range magnetic order. In a recent exact diagonalization study, Cepas *et al.*[24] reached a different conclusion: they claim that there is a nonzero critical DM coupling $D_c$ beyond which magnetic order is induced. They estimate $D_c/J\approx 0.1$, quite close to the value measured[13] for $ZnCu_3(OH)_6Cl_2$ which has $D/J\approx 0.08$. This proximity led Cepas *et al.* to suggest that the quantum criticality of the DM-induced transition to magnetic order controls the observable properties of this kagome antiferromagent.

The purpose of this paper is to propose a theory for the quantum critical point discovered by Cepas *et al.*[24] We will compute various observables of this theory, allowing a potential comparison with numerics and experiments.

Given the evidence for VBS order in the model without DM interactions,[16–19] it would appear we need a theory for the transition from the VBS state to the magnetically ordered state. However, the VBS ordering is weak and can reasonably be viewed as a perturbation on some underlying spin-liquid ground state. Schwandt *et al.*[21] have recently presented evidence that the kagomé antiferromagnet is proximate to a $Z_2$ spin-liquid state, and that vision condensation in this state leads to weak VBS ordering. Their dimer representation leads naturally to $Z_2$ spin-liquid states in the same class as that originally described[27,28] by the Schwinger boson method.[29,30] We will therefore neglect the complexities associated with the VBS ordering and work with the parent $Z_2$ spin-liquid state. This is equivalent to ignoring the physics of the vison sector and assumes that the magnetic-ordering transition can be described in a theory of the spinons alone.[31] The main result of this paper will be a theory of the quantum phase transition from the Schwinger boson $Z_2$ spin liquid to the magnetically ordered state as induced by the DM interactions.

We will begin in Sec. II with a description of the mean-field theory of the $Z_2$ spin liquid and its transition to the magnetically ordered state in the presence of DM interactions. This will be carried using the Sp($N$) Schwinger boson formulation,[27,30] for which the mean-field theory becomes exact in the large $N$ limit. We will turn to fluctuation corrections and the nature of the quantum critical point in Sec. III. Here we will show that the critical theory is the familiar three-dimensional XY model. However, its connection to experimental observables is subtle, in particular, the XY field itself is not directly observable.

While this paper was in preparation, a description of the Schwinger boson mean-field theory in the presence of DM interactions also appeared in Ref. 32; they consider mean-field solutions with larger unit cells than we do, but did not analyze the critical field theory. Where they overlap, our results are in agreement with theirs. We also note the recent experimental observations of Helton *et al.*,[33] who present evidence for quantum criticality in $ZnCu_3(OH)_6Cl_2$.

## II. MEAN-FIELD THEORY

The model we consider is a standard Heisenberg Hamiltonian supplemented by an additional DM interaction. It assumes the form

$$\mathcal{H}=\frac{1}{2}\sum_{i,j}[J_{ij}\mathbf{S_i}\cdot\mathbf{S_j}+\mathbf{D_{ij}}\cdot(\mathbf{S_i}\times\mathbf{S_j})]. \quad (1)$$

$\mathbf{S_i}$ in this notation denotes the spin operator at site $i$, $J_{ij}$ is assumed to be uniform and of the nearest-neighbor type, and

 

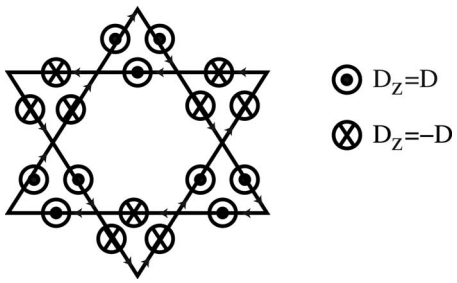


FIG. 1. Staggered DM interaction from triangle to triangle in $z$ direction as in Ref. 34. The arrowheads indicate $D$ to come out of the plane, whereas the tails denote $D$ to go into the plane. Note that the triangles are summed clockwise and anticlockwise, respectively, indicated by the arrows on the bonds.

$\mathbf{D}_{ij}=D_{ij}\mathbf{e}_z$ is taken along the $z$ axis and staggered from triangle to triangle,[34] see Fig. 1.

This additional term explicitly breaks the spin-rotation symmetry by favoring configurations lying in the $x$-$y$ plane. Furthermore this term increases the tendency of classical spin ordering. It has been shown in earlier works[29,30] that Schwinger bosons are ideally suited to describe phase transitions between paramagnetic and magnetically ordered phases in spin models. Following Ref. 27 we introduce a Sp($N$) generalization of the spin operators, which formally allows to consider a controlled large $N$ limit particularly suited for the study of frustrated spin systems such as kagome or triangular antiferromagnets. In the Sp(1) case, which is isomorphic to SU(2), one can represent the spin variables as

$$\mathbf{S}_i = b_{i\sigma}^* \frac{\boldsymbol{\tau}_{\sigma\sigma'}}{2} b_{i\sigma'} \tag{2}$$

with $\vec{\tau}$ being the Pauli matrices and with

$$b_{i\sigma} = \begin{pmatrix} b_{i\uparrow} \\ b_{i\downarrow}^* \end{pmatrix} \quad \text{and} \quad \sum_\sigma b_{i\sigma}^* b_{i\sigma} = 2S = n_b. \tag{3}$$

In the case of the large-$N$ generalization the Schwinger bosons acquire another index counting the copies of the system (we drop this index in the following discussions, but display $N$ whenever it is essential). The large-$N$ generalization formally justifies the mean field with the saddle point becoming exact in the limit $N\to\infty$. In order to properly reformulate the problem at hand we introduce two decoupling parameters

$$Q_{ij} = \sum_{\sigma\sigma'} \epsilon_{\sigma\sigma'} b_{i\sigma} b_{j\sigma'},$$

$$P_{ij} = \sum_{\sigma\sigma'} \tau^x_{\sigma\sigma'} b_{i\sigma} b_{j\sigma'}, \tag{4}$$

where $\epsilon_{\sigma\sigma'}$ is the antisymmetric tensor and $\tau^x$ is just the standard Pauli matrix. We see from the above expressions that $Q_{ij}=-Q_{ji}$ whereas $P_{ij}=P_{ji}$. This implies that the bond variables $P_{ij}$ do not have a direction.

The constraint Eq. (3) is implemented via a Lagrangian multiplier in a standard way. The Hamiltonian of the system formulated in the fields defined in Eq. (4) consequently reads

$$\frac{\mathcal{H}}{N} = -\frac{1}{2}\sum_{i,j} J_{ij} Q_{ij}^* Q_{ij} - \frac{i}{4}\sum_{i,j} D_{ij}(P_{ij}^* Q_{ij} - Q_{ij}^* P_{ij}) + \sum_i \lambda_i (b_{i\sigma}^* b_{i\sigma} - \kappa), \tag{5}$$

where $\kappa=n_b/N$. We furthermore introduce $N_u$ as the number of unit cells in the systems and $N_s$ as the number of sites within the unit cell. We can write the mean-field Hamiltonian per flavor and unit cell as

$$\frac{H_{MF}}{NN_u} = \frac{1}{N_u}\sum_{\mathbf{k}} \Psi^*(\mathbf{k}) \mathbb{H}(q_{ij}, p_{ij}, \lambda, \mathbf{k}) \Psi(\mathbf{k}) + \frac{J}{2}\sum_{(ij)'} |q_{ij}|^2 + \frac{iD}{4}\sum_{(ij)'} (p_{ij}^* q_{ij} - q_{ij}^* p_{ij}) - N_s \lambda (1+\kappa), \tag{6}$$

where $\Sigma_{(ij)'}$ denotes the sum over bonds belonging to the unit cell,

$$\Psi^*(\mathbf{k}) = [b_{1\uparrow}^*(\mathbf{k}), \ldots, b_{N_s\uparrow}^*(\mathbf{k}), b_{1\downarrow}(-\mathbf{k}), \ldots, b_{N_s\downarrow}(-\mathbf{k})] \tag{7}$$

and the matrix

$$\mathbb{H} = \begin{pmatrix} \lambda\mathbb{I} & \mathbb{C}^*(k) \\ \mathbb{C}(k) & \lambda\mathbb{I} \end{pmatrix} \tag{8}$$

with the matrices $\mathbb{I}$ (identity) and $\mathbb{C}(k)$ being $N_s\times N_s$ matrices; the explicit form of these matrices is given in Appendix A. As mentioned before, one of the major assets of the Schwinger boson approach is that it can describe magnetically disordered gapped spin-liquid phases as well as magnetically ordered states. On a formal level in the large $N$ approach this is achieved by introducing the following notation for the Schwinger bosons:

$$b_{i\sigma} = (\sqrt{N} x_i, b_i^{\tilde{m}}) \quad \text{where} \quad \tilde{m} = 2, \ldots, N. \tag{9}$$

The first component is thus a classical field. If $x\neq 0$ it signals condensation which causes long-range order to appear. Following Refs. 27 and 29 we can integrate out the Schwinger bosons and the zero-temperature mean-field energy assumes the following form:

$$\begin{aligned}\frac{E_{MF}}{NN_u} = {} & \frac{1}{N_u}\sum_{\mathbf{k},\mu=1,\ldots,N_s} \omega_\mu(\mathbf{k}) - N_s\lambda(1+\kappa) + \lambda\sum_{i'\sigma} |x_{i\sigma}|^2 \\ & + \frac{J}{2}\sum_{(ij)'} [|q_{ij}|^2 - (q_{ij}^* \epsilon_{\sigma\sigma'} x_{i\sigma} x_{j\sigma'}) + \text{H.c.}) \\ & + \frac{iD}{4}\sum_{(ij)'} (p_{ij}^* q_{ij} - q_{ij}^* p_{ij}) - \frac{iD}{4}\sum_{(ij)'} (p_{ij}^* \epsilon_{\sigma\sigma'} x_{i\sigma} x_{j\sigma'} \\ & + q_{ij} \tau^x_{\sigma\sigma'} x_{i\sigma}^* x_{j\sigma'}^*) + \frac{iD}{4}\sum_{(ij)'} (p_{ij} \epsilon_{\sigma\sigma'} x_{i\sigma}^* x_{j\sigma'}^* \\ & + q_{ij}^* \tau^x_{\sigma\sigma'} x_{i\sigma} x_{j\sigma'}),\end{aligned} \tag{10}$$

where $\Sigma_{i'}$ denotes the sum over all sites within one unit cell.

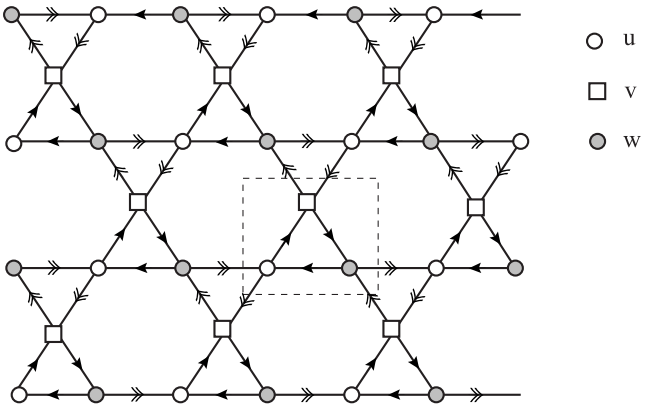


FIG. 2. We take a unit cell of three sites, labeled $u$, $v$, and $w$. The arrows indicate the values of the oriented variables $q_{ij}$. The links with single arrows have $q_{ij}=q_1$, while those with double arrows have $q_{ij}=q_2$. The $P_{ij}$ are unoriented and take values $p_1$ and $p_2$ on these links, respectively.

In the following we solve the self-consistency equations according to

$$\kappa = \langle b_{i\sigma}^{*} b_{i\sigma} \rangle_{MF},$$

$$q_{ij} = \langle Q_{ij} \rangle_{MF},$$

$$p_{ij} = \langle P_{ij} \rangle_{MF} \tag{11}$$

with the Hamiltonian defined in Eq. (6).

Our solution of the mean-field equations follows previous work,[27,28] which classified physically different $Z_2$ spin-liquid solutions without the DM interactions. We found that these solutions have a natural generalization in the presence of DM terms with values of the $p_{ij}$ which reflect the symmetries of the $q_{ij}$. Two stable solutions were found in previous work with only two possibly distinct values of $q_{ij}$ as illustrated in Fig. 2. Including the DM interactions, these solutions extended to:

(i) $q_1=q_2$ real, $p_1=p_2$ pure imaginary: upon increasing $\kappa$, the Schwinger bosons condense at $\mathbf{k}=0$ with the spins at angles of 120° to each other within the unit cell. This state is therefore called the $\mathbf{k}=0$ state.

(ii) $q_1=-q_2$ real, $p_1=-p_2$ pure imaginary: upon increasing $\kappa$, the Schwinger bosons condense at wave vector $\mathbf{k}=\pm(2\pi/3,0)$ into a state which is called the $\sqrt{3}\times\sqrt{3}$ antiferromagnet, characterized by an enlarged unit cell. Solutions with larger unit cells can be present with additional frustrating interactions,[28] but we will not consider them here.

### Phase diagram

Our phase diagram is shown in Fig. 3 as a function of $\kappa=n_b/N$ (which corresponds to the spin size) and the parameter $D/J$. Our phase diagram is similar to that obtained recently by Messio *et al.*[32] They also considered solutions with a larger unit cell which were stable over some portion of the phase diagram.

We start with a discussion of the classical limit. While for $D=0$ the long-range ordered state of the $\sqrt{3}\times\sqrt{3}$ type is generically preferred,[27] infinitesimal $D$ favors the so-called $\mathbf{k}=0$ state. This is reproduced by our mean-field equations in the large spin limit $\kappa\to\infty$. For finite values of $\kappa$ there is a small slab in which long-range order of the $\sqrt{3}\times\sqrt{3}$ type is favored over the $\mathbf{k}=0$. These states are separated by a first-order transition driven by the ratio $D/J$.

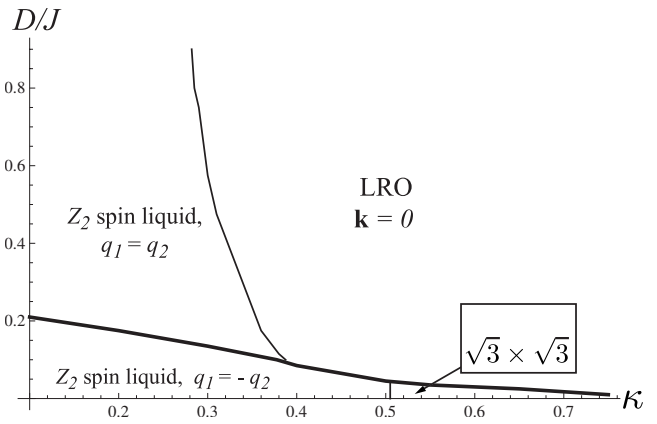


FIG. 3. Phase diagram in the $N\to\infty$ limit of the Sp($N$) theory. The $x$ axis shows $\kappa=2S/N$ and the $y$ axis $D/J$. The phases have long-range magnetic order type (LRO) or gapped $Z_2$ spin liquids. The thick line is a first-order transition while the thin lines are second-order transitions: the transition to the $\mathbf{k}=0$ LRO state is described in Sec. III. The limit of $D/J\to 0$ reduces to the results presented in Ref. 27.

A similar behavior appears for the corresponding spin-liquid states at small $\kappa$. The $q_1=-q_2$ is favored at small $D/J$ and then undergoes a first-order transition to the $q_1=q_2$ state at large $D/J$.

In exact diagonalization studies of the spin $S=\frac{1}{2}$ kagome antiferromagnet with DM interactions a second-order phase transition between a phase with short-ranged $\mathbf{k}=0$ correlations[18,35] (obtained in the pure Heisenberg case) and phase with $\mathbf{k}=0$ long-range order was found.[32] Such a transition is also present in our mean-field theory, which therefore can be used for a study of critical properties in Sec. III.

## III. QUANTUM CRITICALITY

We will consider only the transition out of the $q_1=q_2$ spin liquid, because that is what is seen in the numerical studies.[24] The corresponding transition out of the $q_1=-q_2$ spin liquid can be treated in a similar manner. Throughout this section we will consider the physical SU(2) antiferromagnet directly and not take the large $N$ limit. The method followed below has been reviewed in a more general context in Ref. 30.

Since we are at $\mathbf{k}=0$, we can write the effective action for the bosons by making the small momentum expansion of the matrix in Eq. (A2). We take three sites, $u$, $v$, and $w$, in each unit cell (see Fig. 2), and then take the continuum limit of the saddle-point Lagrangian. We write the boson operators on these sites as $b_{u\sigma}=U_\sigma$, $b_{v\sigma}=V_\sigma$, etc., and set $q_1=q_2=q$ and $p_1=p_2=ip$ with $q$ and $p$ real. Then, we write the final Lagrangian in the form

$$\mathcal{L} = \mathcal{L}_H + \mathcal{L}_{\mathrm{DM}} \tag{12}$$

representing the contributions of the Heisenberg exchange and the DM coupling, respectively.

From Eq. (A2) we obtain the Lagrangian in the absence of a DM term (which describes the $\mathbf{k}=0$ solution of Ref. 27)

$$\mathcal{L}_H = U_\sigma^* \frac{\partial U_\sigma}{\partial \tau} + V_\sigma^* \frac{\partial V_\sigma}{\partial \tau} + W_\sigma^* \frac{\partial W_\sigma}{\partial \tau} + \lambda(|U_\sigma|^2 + |V_\sigma|^2 + |W_\sigma|^2) - Jq\epsilon_{\sigma\sigma'}(U_\sigma V_{\sigma'} + V_\sigma W_{\sigma'} + W_\sigma U_{\sigma'}) + \text{c.c.} + \frac{Jq}{2}\epsilon_{\sigma\sigma'}(\partial_1 U_\sigma \partial_1 V_{\sigma'} + \partial_2 V_\sigma \partial_2 W_{\sigma'} + \partial_3 W_\sigma \partial_3 U_{\sigma'}) + \text{c.c.}, \tag{13}$$

where $\partial_i$ is the gradient along the direction $\mathbf{e}_i$ in Eq. (A1).

We now perform a unitary transformation to new variables $X_\sigma$, $Y_\sigma$, and $Z_\sigma$. These are chosen to diagonalize only the nongradient terms in $\mathcal{L}_H$.

$$\begin{pmatrix} U_\sigma \\ V_\sigma \\ W_\sigma \end{pmatrix} = \frac{Z_\sigma}{\sqrt{6}}\begin{pmatrix} 1 \\ \zeta \\ \zeta^2 \end{pmatrix} + \epsilon_{\sigma\sigma'}\frac{Z_{\sigma'}^*}{\sqrt{6}}\begin{pmatrix} i \\ i\zeta^2 \\ i\zeta \end{pmatrix} + \frac{Y_\sigma}{\sqrt{6}}\begin{pmatrix} 1 \\ \zeta \\ \zeta^2 \end{pmatrix} + \epsilon_{\sigma\sigma'}\frac{Y_{\sigma'}^*}{\sqrt{6}}\begin{pmatrix} -i \\ -i\zeta^2 \\ -i\zeta \end{pmatrix} + \frac{X_\sigma}{\sqrt{3}}\begin{pmatrix} 1 \\ 1 \\ 1 \end{pmatrix}, \tag{14}$$

where $\zeta \equiv e^{2\pi i/3}$. The tensor structure above makes it clear that this transformation is rotationally invariant, and that $X_\sigma$, $Y_\sigma$, and $Z_\sigma$ transform as spinors under SU(2) spin rotations. Inserting Eq. (14) into $\mathcal{L}_H$ we find

$$\mathcal{L}_H = X_\sigma^* \frac{\partial X_\sigma}{\partial \tau} + Y_\sigma^* \frac{\partial Z_\sigma}{\partial \tau} + Z_\sigma^* \frac{\partial Y_\sigma}{\partial \tau} + (\lambda + \sqrt{3}Jq)|Z_\sigma|^2 + (\lambda - \sqrt{3}Jq)|Y_\sigma|^2 + \lambda|X_\sigma|^2 + \frac{Jq\sqrt{3}}{2}(|\partial_x Z_\sigma|^2 + |\partial_y Z_\sigma|^2) + \cdots. \tag{15}$$

The ellipses indicate omitted terms involving spatial gradients in the $X_\sigma$ and $Y_\sigma$ which we will not keep track of. This is because the fields $Y_\sigma$ and $X_\sigma$ are massive relative to $Z_\sigma$ (for $q<0$ which is the case in our mean-field solution), and so can be integrated out. This yields the effective Lagrangian

$$\mathcal{L}_H^Z = \frac{1}{(\lambda - \sqrt{3}Jq)}|\partial_\tau Z_\sigma|^2 + \frac{Jq\sqrt{3}}{2}(|\partial_x Z_\sigma|^2 + |\partial_y Z_\sigma|^2) + (\lambda + \sqrt{3}Jq)|Z_\sigma|^2 + \cdots. \tag{16}$$

Note that the omitted spatial gradient terms in $X_\sigma$ and $Y_\sigma$ do contribute a correction to the spatial gradient term in Eq. (16), and we have not accounted for this. This Lagrangian shows that the mean-field theory has a transition to magnetic order at $\lambda = |\sqrt{3}Jq|$, which agrees with earlier results.[27]

The effective Lagrangian $\mathcal{L}_H^Z$ is almost the complete solution for the critical theory in the system without the DM interactions. However, we also need higher order terms in Eq. (16), which will arise from including the fluctuations of the gapped fields $Q$ and $\lambda$. Rather than computing these from the microscopic Lagrangian, it is more efficient to deduce their structure from symmetry considerations. The representation in Eq. (14), and the connection of the $U$, $V$, and $W$ to the lattice degrees of freedom, allow us to deduce the following symmetry transformations of the $X$, $Y$, and $Z$.

(1) Under a global spin rotation by the SU(2) matrix $g_{\sigma\sigma'}$, we have $Z_\sigma \to g_{\sigma\sigma'}Z_{\sigma'}$, and similarly for $Y$ and $Z$. When DM interactions are included, the global symmetry is reduced to U(1) rotations about the $z$ axis, under which

$$Z_\uparrow \to e^{i\theta}Z_\uparrow, \quad Z_\downarrow \to e^{-i\theta}Z_\downarrow,$$
$$Y_\uparrow \to e^{i\theta}Y_\uparrow, \quad Y_\downarrow \to e^{-i\theta}Y_\downarrow,$$
$$X_\uparrow \to e^{i\theta}X_\uparrow, \quad X_\downarrow \to e^{-i\theta}X_\downarrow. \tag{17}$$

(2) Under a 120° lattice rotation, we have $U_\sigma \to V_\sigma$, $V_\sigma \to W_\sigma$, and $W_\sigma \to U_\sigma$. From Eq. (14), we see that this symmetry is realized by

$$Z_\sigma \to \zeta Z_\sigma, \quad Y_\sigma \to \zeta Y_\sigma, \quad X_\sigma \to X_\sigma. \tag{18}$$

Note that this is distinct from the SU(2) rotation because $\det(\zeta) \neq 1$.

(3) Under time reversal, we have $U_\sigma \to \epsilon_{\sigma\sigma'}U_{\sigma'}^*$ and similarly for $V_\sigma$ and $W_\sigma$. This is realized in Eq. (14) by

$$Z_\sigma \to iZ_\sigma, \quad Y_\sigma \to -iY_\sigma, \quad X_\sigma \to \epsilon_{\sigma\sigma'}X_{\sigma'}^*. \tag{19}$$

In particular, note that $Z_\uparrow$ does not map to $Z_\downarrow$ under time reversal.

It is easy to verify that Eq. (15) is invariant under all the symmetry operations above. These symmetry operators make it clear that the only allowed quartic term for the Heisenberg Hamiltonian is $(\Sigma_\sigma|Z_\sigma|^2)^2$: this implies that the $Z_2$ spin liquid to antiferromagnetic order transition of this model is in the universality class of the O(4) model.[37]

Let us now include the DM interactions. From Eq. (A2), we see that

$$\mathcal{L}_{\text{DM}} = i\frac{Dq}{2}\tau^x_{\sigma\sigma'}(U_\sigma V_{\sigma'} + V_\sigma W_{\sigma'} + W_\sigma U_{\sigma'}) + \text{c.c.} \tag{20}$$

We have dropped a term proportional to $Dp$, which has the same structure as the terms in Eq. (15), and ignored spatial gradients. In terms of the fields in Eq. (14), this takes the simple form

$$\mathcal{L}_{\text{DM}} = \frac{Dq}{2}(i\tau^x_{\sigma\sigma'}X_\sigma X_{\sigma'} + \text{c.c.} - Z_\sigma^*\tau^z_{\sigma\sigma'}Z_{\sigma'} + Y_\sigma^*\tau^z_{\sigma\sigma'}Y_{\sigma'}), \tag{21}$$

and it can be verified that these terms are invariant under Eqs. (17)–(19). As before, we now integrate out $X_\sigma$ and $Y_\sigma$ from $\mathcal{L}_H + \mathcal{L}_{\text{DM}}$ in Eqs. (15) and (21). We obtain a Lagrangian with the same structure as Eq. (16), but all couplings become dependent on $\sigma$; in other words, we have two separate XY models for $Z_\uparrow$ and $Z_\downarrow$. Performing a careful analysis of allowed higher order terms as restricted by the symmetry constraints discussed above, and after appropriate rescalings of the spatial, temporal, and field scales, we obtain the field theory with the Lagrangian

$$\mathcal{L}_Z = |\partial_\tau Z_\uparrow|^2 + |\boldsymbol{\nabla} Z_\uparrow|^2 + s_\uparrow |Z_\uparrow|^2 + u_\uparrow |Z_\uparrow|^4 + |\partial_\tau Z_\downarrow|^2 + |\boldsymbol{\nabla} Z_\downarrow|^2 + s_\downarrow |Z_\downarrow|^2 + u_\downarrow |Z_\downarrow|^4 + v|Z_\uparrow|^2 |Z_\downarrow|^2 + w[(Z_\uparrow Z_\downarrow)^6 + (Z_\uparrow^* Z_\downarrow^*)^6]. \tag{22}$$

Note that $s_\uparrow \neq s_\downarrow$, in general (and similarly for $u_{\uparrow,\downarrow}$, etc.), and equality is not required by the time-reversal symmetry in Eq. (19). Time-reversal symmetry does prohibit a term $\sim(Z_\uparrow Z_\downarrow)^3$ which is allowed by the other symmetries. Thus we expect only one of $Z_\uparrow$ or $Z_\downarrow$ to condense at the quantum critical point: as we will see from the analysis of observables in Sec. III A, this transition does indeed correspond to the development of spiral magnetic order in the $x$-$y$ plane. The choice between $Z_\uparrow$ and $Z_\downarrow$ is controlled by the sign of $D$.

Equation (22) also contains terms which couple the two XY models to each other. The lowest allowed term, $v$, couples the energy densities and does not have any important effects. More interesting is the $w$ term, which shows that the global symmetry is not $\mathrm{O}(2)\otimes\mathrm{O}(2)$ but $\mathrm{O}(2)\otimes\mathbb{Z}_{12}$. In the magnetically ordered phase with $\langle Z_\uparrow\rangle \neq 0$ (say), this term will induce a small ordering field $\sim Z_\downarrow^6$ in the XY model for $Z_\downarrow$. However, the action for $Z_\downarrow$ has a "mass" term $s_\downarrow$ with a positive coefficient, and this sixth-order term will not immediately induce ordering in $Z_\downarrow$, i.e., a magnetic phase with $\langle Z_\uparrow\rangle \neq 0$ and $\langle Z_\downarrow\rangle = 0$ has a finite range of stability. Thus close to the transition we can neglect the $Z_\downarrow$ field entirely and transition is in the universality class of the three-dimensional XY model.

The choice above of $Z_\uparrow$ over $Z_\downarrow$ gives the incorrect appearance that we are breaking the spin-reflection symmetry $S_z \to -S_z$ of $\mathcal{H}$, suggesting the appearance of a net $z$ ferromagnetic moment. However, notice that the theory of $Z_\uparrow$ is relativistic, and so contains both spinons and antispinons which carry $S_z = +1/2$ and $S_z = -1/2$, respectively. The spinon of $Z_\downarrow$ also carries $S_z = -1/2$, and this is degenerate with the antispinon of $Z_\uparrow$ in the O(4) invariant theory in Eq. (16). It is this latter degeneracy which is lifted by the DM interactions, which induce a vector spin chirality along the $z$ direction[36] (as we will see below). We will also see there is no net ferromagnetic moment, because time-reversal symmetry is preserved.

### A. Observables

To determine the operators corresponding to the ferromagnetic moment, let us couple a uniform external field $\mathbf{h}$ to the lattice Hamiltonian. This adds to the continuum Lagrangian the term

$$\mathcal{L}_h = -\mathbf{h}\cdot\boldsymbol{\tau}_{\sigma\sigma'}(U_\sigma^* U_{\sigma'} + V_\sigma^* V_{\sigma'} + W_\sigma^* W_{\sigma'}). \tag{23}$$

Inserting the parameterization in Eq. (14) this becomes

$$\mathcal{L}_h = -\mathbf{h}\cdot\boldsymbol{\tau}_{\sigma\sigma'}(X_\sigma^* X_{\sigma'} + Y_\sigma^* Z_{\sigma'} + Z_\sigma^* Y_{\sigma'}). \tag{24}$$

We now need to integrate out $X_\sigma$ and $Y_\sigma$ in the Lagrangian $\mathcal{L}_H + \mathcal{L}_{\mathrm{DM}} + \mathcal{L}_h$ defined by the sum of Eqs. (15), (21), and (24) and collect the terms linear in $\mathbf{h}$. Without the DM coupling, we obtain

$$\sim \mathbf{h}\cdot\boldsymbol{\tau}_{\sigma\sigma'}\left(Z_\sigma^* \frac{\partial Z_{\sigma'}}{\partial\tau} - \frac{\partial Z_\sigma^*}{\partial\tau} Z_{\sigma'}\right). \tag{25}$$

Comparing with $\mathcal{L}_H^Z$ in Eq. (16) we see that this is just the coupling to the conserved SU(2) charges of the O(4) model: this is the usual term which determines the magnetic susceptibility of the Heisenberg antiferromagnet.[37] Upon including the effects of $\mathcal{L}_{\mathrm{DM}}$ we find that the essential structure of Eq. (25) does not change: the $\boldsymbol{\tau}$ matrices get multiplied by some $\sigma$-dependent factors $\boldsymbol{\tau}_{\sigma\sigma'} \to f_\sigma \boldsymbol{\tau}_{\sigma\sigma'} f_{\sigma'}$ which do not modify the scaling considerations. No term with a new structure is generated by the DM coupling. It can now be seen that these expressions have vanishing expectation values under $\mathcal{L}_Z$ in Eq. (22), and so there is no net ferromagnetic moment in the absence of an external field.

We now turn to the antiferromagnetic order parameter; for a coplanar antiferromagnet, this is described by

$$\mathbf{S}_i \propto \mathbf{N}_1 \cos(\mathbf{Q}\cdot\mathbf{r}_i) + \mathbf{N}_2 \sin(\mathbf{Q}\cdot\mathbf{r}_i), \tag{26}$$

where $\mathbf{N}_{1,2}$ are two orthogonal vectors representing the spiral order and $\mathbf{Q}$ is wave vector at which the spin structure factor is peaked. For our model, we can see that

$$\mathbf{N}_1 + i\mathbf{N}_2 = \mathbf{S}_u + \zeta \mathbf{S}_v + \zeta^2 \mathbf{S}_w. \tag{27}$$

Using Eq. (14), and keeping only the lowest order term, we therefore obtain[37]

$$\mathbf{N}_1 + i\mathbf{N}_2 = \begin{pmatrix} i(Z_\uparrow^2 - Z_\downarrow^2)/2 \\ -(Z_\uparrow^2 + Z_\downarrow^2)/2 \\ -iZ_\uparrow Z_\downarrow \end{pmatrix}, \tag{28}$$

in a notation that makes the rotational invariance evident, this relationship is

$$\mathbf{N}_1 + i\mathbf{N}_2 = \frac{i}{2}\boldsymbol{\epsilon}_{\alpha\beta}\boldsymbol{\tau}_{\beta\sigma} Z_\sigma Z_\alpha. \tag{29}$$

Note that a phase with $\langle Z_\uparrow\rangle \neq 0$ and $\langle Z_\downarrow\rangle = 0$ has spiral order in the $x$-$y$ plane.

To complete the list of operators which are quadratic in the $Z_\sigma$, we consider the vector spin chirality.[36] This is defined here by

$$\mathbf{S}_u \times \mathbf{S}_v + \mathbf{S}_v \times \mathbf{S}_w + \mathbf{S}_w \times \mathbf{S}_u. \tag{30}$$

Using Eq. (14) we find that the leading operator mapping to vector spin chirality is (dropping an overall factor of $|Z_\uparrow|^2 + |Z_\downarrow|^2$)

$$Z_\sigma^* \boldsymbol{\tau}_{\sigma\sigma'} Z_{\sigma'}. \tag{31}$$

Note that in the presence of the DM term, the couplings in the effective theory Eq. (22) imply that the $z$ component of the vector spin chirality is always nonzero.

### B. Critical properties

Let us assume the transition to magnetic order proceeds via the condensation of $Z_\uparrow$. The transition is in the XY universality class, and the dimension of the antiferromagnetic order parameter is

$$\dim[\mathbf{N}_1] = \dim[\mathbf{N}_2] = \dim[Z_\uparrow^2] = \frac{1+\bar{\eta}}{2}. \tag{32}$$

The value of the exponent $\bar{\eta}$ can be read off from results for the three-dimensional XY model,[38,39] and we obtain $\bar{\eta} \approx 1.474$. The antiferromagnetic susceptibility will diverge at the critical point as $T^{-(2-\bar{\eta})}$. We note the recent work of Ref. 40 in a different context, which also considered a model with an XY critical point at which the physically measurable magnetic order was the square of the XY field.

The behavior of the uniform magnetic susceptibility follows from the scaling dimension of the operators in Eq. (25). For **h** along the $z$ direction, the magnetization is the just the conserved U(1) charge of the XY model: so[41] it has scaling dimension two and the susceptibility $\sim T$. For **h** along the $x$ or $y$ directions, we have to integrate out $Z_\downarrow$, and then the lowest dimension operator coupling to the square of the field is $|Z_\uparrow|^2$. This means that the susceptibility only has a weak singularity at the quantum critical point given by that in $\langle |Z_\uparrow|^2 \rangle$: at the quantum critical point, there is a nonanalytic term $\sim T^{3-1/\nu}$, above an analytic background.

## IV. CONCLUSION

We have presented a theory for the quantum critical point between a $Z_2$ spin liquid and an ordered antiferromagnet for the kagomé antiferromagnet in the presence of DM interactions. The critical theory is just the three-dimensional XY model. However, the XY order parameter carries a $Z_2$ gauge charge, and so it is not directly observable. In particular, the antiferromagnetic order parameter is the square of the XY order parameter. Specifically, the theory is given by $\mathcal{L}_Z$ in Eq. (22), and its observables are described in Sec. III A.

It is interesting to compare our results with recent observations of quantum critical scaling in $ZnCu_3(OH)_6Cl_2$ by Helton *et al.*[33] Their neutron-scattering measurements show an antiferromagnetic susceptibility which scales as $T^{-0.66}$. This is actually in reasonable agreement with our theory, which has a susceptibility $\sim T^{-0.526}$. However, they also observe a similar divergence in measurements of the uniform magnetization, while our theory only predicts a very weak singularity. We suspect that this difference is due to the present of impurities,[6–9,15,42] which can mix the uniform and staggered components. A complete study of impurities near the quantum critical point described above is clearly called for.

## ACKNOWLEDGMENTS

We thank L. Messio, O. Cépas, C. Lhuillier, and E. Vicari for useful discussions. This research was supported by the National Science Foundation under Grant No. DMR-0757145, by the FQXi foundation, and by a MURI grant from AFOSR. Y.H. is also supported in part by a Samsung scholarship.

## APPENDIX A: MICROSCOPIC FORM OF THE HAMILTONIAN

We here give explicit expressions for the Hamiltonian introduced in Sec. II. We introduce the following set of unit vectors:

$$\mathbf{e}_1 = a\left(\frac{1}{2}, \frac{\sqrt{3}}{2}\right),$$

$$\mathbf{e}_2 = a\left(\frac{1}{2}, -\frac{\sqrt{3}}{2}\right),$$

$$\mathbf{e}_3 = a(-1, 0), \tag{A1}$$

which allows to express $k_i = \mathbf{k}\cdot\mathbf{e}_i$. In the following we concentrate on the states with three sites per unit cell. In that case the vector $\Psi$ introduced in Eq. (7) has six components and the matrix $\mathbb{C}$ consequently is a $3\times 3$ matrix with the following entries:

$$\mathbb{C}_{uv} = \frac{J}{2}q_1^* e^{ik_1} + \frac{J}{2}q_2^* e^{-ik_1} + \frac{iD}{4}p_1^* e^{ik_1} + \frac{iD}{4}q_1^* e^{ik_1} + \frac{iD}{4}p_2^* e^{-ik_1} + \frac{iD}{4}q_2^* e^{-ik_1},$$

$$\mathbb{C}_{uw} = -\frac{J}{2}q_1^* e^{-ik_3} - \frac{J}{2}q_2^* e^{ik_3} - \frac{iD}{4}p_1^* e^{-ik_3} + \frac{iD}{4}q_1^* e^{-ik_3} - \frac{iD}{4}p_2^* e^{ik_3} + \frac{iD}{4}q_2^* e^{ik_3},$$

$$\mathbb{C}_{vw} = \frac{J}{2}q_1^* e^{ik_2} + \frac{J}{2}q_2^* e^{-ik_2} + \frac{iD}{4}p_1^* e^{ik_2} + \frac{iD}{4}q_1^* e^{ik_2} + \frac{iD}{4}p_2^* e^{-ik_2} + \frac{iD}{4}q_2^* e^{-ik_2},$$

$$\mathbb{C}_{vu} = -\frac{J}{2}q_1^* e^{-ik_1} - \frac{J}{2}q_2^* e^{ik_1} - \frac{iD}{4}p_1^* e^{-ik_1} + \frac{iD}{4}q_1^* e^{-ik_1} - \frac{iD}{4}p_2^* e^{ik_1} + \frac{iD}{4}q_2^* e^{ik_1},$$

$$\mathbb{C}_{wv} = -\frac{J}{2}q_1^* e^{-ik_2} - \frac{J}{2}q_2^* e^{ik_2} - \frac{iD}{4}p_1^* e^{-ik_2} + \frac{iD}{4}q_1^* e^{-ik_2} - \frac{iD}{4}p_2^* e^{ik_2} + \frac{iD}{4}q_2^* e^{ik_2},$$

$$\mathbb{C}_{wu} = \frac{J}{2}q_1^* e^{ik_3} + \frac{J}{2}q_2^* e^{-ik_3} + \frac{iD}{4}p_1^* e^{ik_3} + \frac{iD}{4}q_1^* e^{ik_3} + \frac{iD}{4}p_2^* e^{-ik_3} + \frac{iD}{4}q_2^* e^{-ik_3}. \tag{A2}$$

## APPENDIX B: DISPERSION OF THE LOWEST EXCITED SPINON STATE

For $q_1 = q_2$ and $D=0$, the ground state is doubly degenerate. The degeneracy splits as $D$ moves away from 0. In all cases, the minimum excitation energy occurs at $\mathbf{k}=0$.

Figure 4 plots the momentum dependence of the energy of the lowest excited spinon at $D/J=0.3$, $\kappa=0.2$. There is a

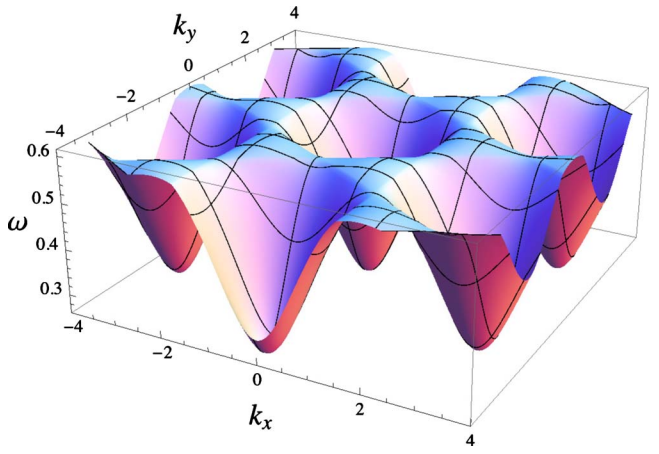


FIG. 4. (Color online) Momentum dependence of the energy $\omega(k)$ of the lowest excited spinon state of the kagome-lattice quantum antiferromagnet for the $q_1=q_2$ state at $D/J=0.3$, $\kappa=0.2$. The minimum excitation energy is at $\mathbf{k}=0$ and has a finite energy gap.

finite energy gap at $\mathbf{k}=0$ making it a gapped spin liquid. On the other hand, Fig. 5 is the dispersion plot for a case with long-range magnetic order. The energy gap at $\mathbf{k}=0$ is closed and condensation occurs at this wave vector.

For $q_1=-q_2$, there is a unique ground state even for $D=0$. Energy minima is at $\mathbf{k}=\pm(2\pi/3,0)$. Figure 6 shows the dispersion of the lowest lying state of the spin liquid with $D/J=0.03$, $\kappa=0.55$. A case with long-range ordering is shown in Fig. 7.

## APPENDIX C: CONDENSATION

For the $q_1=q_2$ state Eq. (14) leads to the following parametrization of the condensation of $Z_\downarrow$ field at $\mathbf{k}=0$:

$$\begin{pmatrix} x_u^\uparrow \\ x_u^\downarrow \end{pmatrix} = \ell \begin{pmatrix} i \\ 1 \end{pmatrix},$$

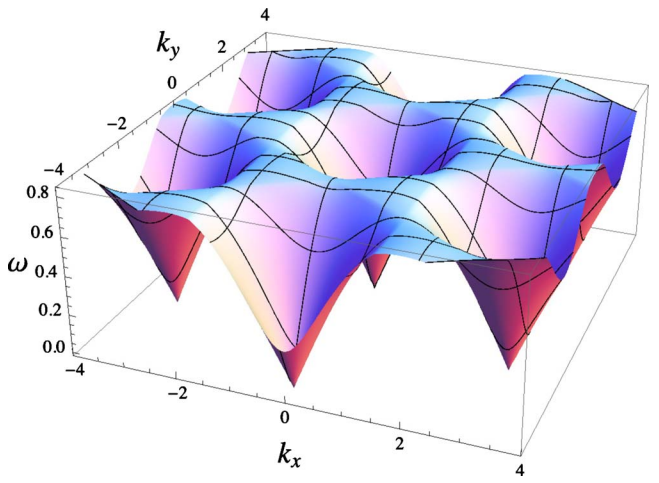


FIG. 5. (Color online) Dispersion of the lowest excited spinon state for the $q_1=q_2$ state at $D/J=0.3$, $\kappa=0.4$. The energy gap closes at $\mathbf{k}=0$ and condensation occurs.

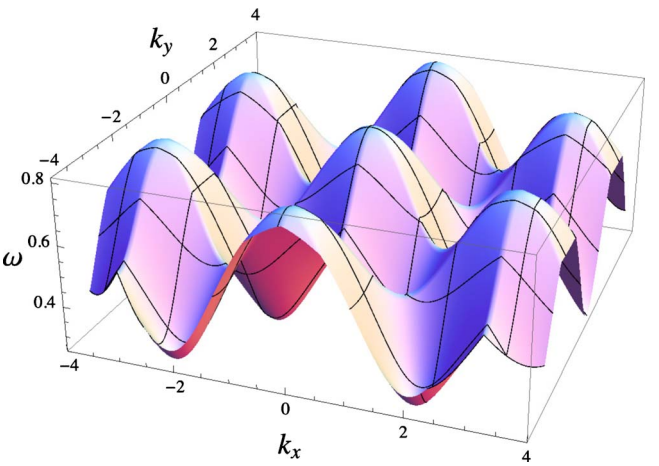


FIG. 6. (Color online) Disorder: $q_1=-q_2$, $D/J=0.05$, $\kappa=0.3$.

$$\begin{pmatrix} x_v^\uparrow \\ x_v^\downarrow \end{pmatrix} = \ell \begin{pmatrix} i\zeta^2 \\ \zeta \end{pmatrix},$$

$$\begin{pmatrix} x_w^\uparrow \\ x_w^\downarrow \end{pmatrix} = \ell \begin{pmatrix} i\zeta \\ \zeta^2 \end{pmatrix}, \tag{C1}$$

where $\ell$ is the size of the condensate. Condensation of $Z_\uparrow$ can be written similarly. For $D>0$, $Z_\downarrow$ field condensation is energetically favored while the opposite is true for $D<0$. The two condensations are degenerate for $D=0$.

For the $q_1=-q_2$ state, condensation occurs at $\tilde{k}\equiv\vec{k}=(2\pi/3,0)$ or $\vec{k}=-\tilde{k}$. The two states have identical energies and the condensation is spontaneously chosen. Similar analysis to Eqs. (13) and (14) gives the eigenvectors corresponding to the lowest lying state. For $\vec{k}=\tilde{k}$ this is $(i,-i,i,1,-1,1)$ while for $\vec{k}=-\tilde{k}$ the corresponding eigenvector is $(-i,i,-i,1,-1,1)$. Therefore condensations can be parametrized as

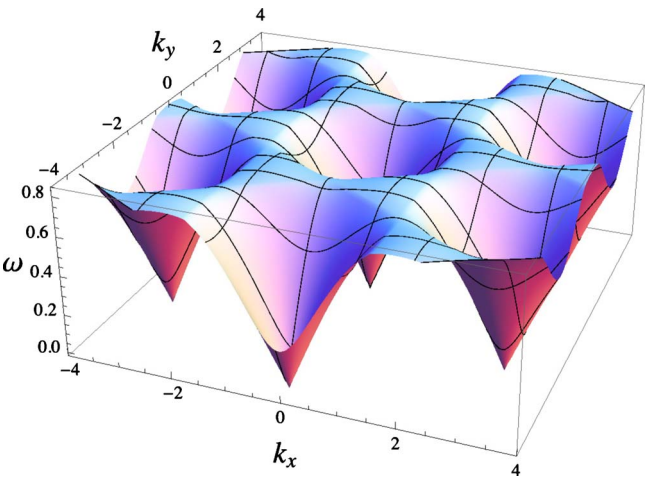


FIG. 7. (Color online) Order: $q_1=-q_2$, $D/J=0.03$, $\kappa=0.55$.

$$\begin{pmatrix} x^u_{k\uparrow} \\ x^u_{-k\downarrow} \end{pmatrix} = \ell \begin{pmatrix} i \\ 1 \end{pmatrix},$$

$$\begin{pmatrix} x^v_{k\uparrow} \\ x^v_{-k\downarrow} \end{pmatrix} = \ell \begin{pmatrix} -i \\ -1 \end{pmatrix},$$

$$\begin{pmatrix} x^w_{k\uparrow} \\ x^w_{-k\downarrow} \end{pmatrix} = \ell \begin{pmatrix} i \\ 1 \end{pmatrix} \quad \text{(C2)}$$

for $\vec{k}=\tilde{k}$ and

$$\begin{pmatrix} x^u_{k\uparrow} \\ x^u_{-k\downarrow} \end{pmatrix} = \ell \begin{pmatrix} -i \\ 1 \end{pmatrix},$$

$$\begin{pmatrix} x^v_{k\uparrow} \\ x^v_{-k\downarrow} \end{pmatrix} = \ell \begin{pmatrix} i \\ -1 \end{pmatrix},$$

$$\begin{pmatrix} x^w_{k\uparrow} \\ x^w_{-k\downarrow} \end{pmatrix} = \ell \begin{pmatrix} -i \\ 1 \end{pmatrix} \quad \text{(C3)}$$

for $\vec{k}=-\tilde{k}$.


[1] J. S. Helton, K. Matan, M. P. Shores, E. A. Nytko, B. M. Bartlett, Y. Yoshida, Y. Takano, A. Suslov, Y. Qiu, J.-H. Chung, D. G. Nocera, and Y. S. Lee, Phys. Rev. Lett. **98**, 107204 (2007).
[2] O. Ofer, A. Keren, E. Nytko, M. Shores, B. Bartlett, D. Nocera, C. Baines, and A. Amato, arXiv:cond-mat/0610540 (unpublished).
[3] P. Mendels, F. Bert, M. A. de Vries, A. Olariu, A. Harrison, F. Duc, J. C. Trombe, J. S. Lord, A. Amato, and C. Baines, Phys. Rev. Lett. **98**, 077204 (2007).
[4] T. Imai, E. A. Nytko, B. M. Bartlett, M. P. Shores, and D. G. Nocera, Phys. Rev. Lett. **100**, 077203 (2008).
[5] S. Dommange, M. Mambrini, B. Normand, and F. Mila, Phys. Rev. B **68**, 224416 (2003).
[6] S.-H. Lee, H. Kikuchi, Y. Qiu, B. Lake, Q. Huang, K. Habicht, and K. Kiefer, Nat. Mater. **6**, 853 (2007).
[7] A. Olariu, P. Mendels, F. Bert, F. Duc, J.-C. Trombe, M. A. de Vries, and A. Harrison, Phys. Rev. Lett. **100**, 087202 (2008).
[8] K. Gregor and O. I. Motrunich, Phys. Rev. B **77**, 184423 (2008).
[9] M. J. Rozenberg and R. Chitra, Phys. Rev. B **78**, 132406 (2008).
[10] I. Dzyaloshinsky, J. Phys. Chem. Solids **4**, 241 (1958).
[11] T. Moriya, Phys. Rev. **120**, 91 (1960).
[12] M. Rigol and R. R. P. Singh, Phys. Rev. Lett. **98**, 207204 (2007).
[13] A. Zorko, S. Nellutla, J. van Tol, L. C. Brunel, F. Bert, F. Duc, J.-C. Trombe, M. A. de Vries, A. Harrison, and P. Mendels, Phys. Rev. Lett. **101**, 026405 (2008).
[14] O. Ofer and A. Keren, Phys. Rev. B **79**, 134424 (2009).
[15] I. Rousochatzakis, S. R. Manmana, A. M. Läuchli, B. Normand, and F. Mila, Phys. Rev. B **79**, 214415 (2009).
[16] P. Nikolic and T. Senthil, Phys. Rev. B **68**, 214415 (2003).
[17] R. R. P. Singh and D. A. Huse, Phys. Rev. B **76**, 180407(R) (2007).
[18] H. C. Jiang, Z. Y. Weng, and D. N. Sheng, Phys. Rev. Lett. **101**, 117203 (2008).
[19] G. Evenbly and G. Vidal, arXiv:0904.3383 (unpublished).
[20] K. Shapiro, J. Falconbarroso, G. Vandeven, P. Dezeeuw, M. Sarzi, R. Bacon, A. Bolatto, M. Cappellari, D. Croton, R. Davies, E. Emsellem, O. Fakhouri, D. Krajnovic, H. Kuntschner, R. Mcdermid, R. Peletier, R. Vandenbosch, and G. Vanderwolk, arXiv:0912.0274, Mon. Not. R. Astron. Soc. (to be published).
[21] D. Schwandt, M. Mambrini, and D. Poilblanc, arXiv:1002.0774 (unpublished).
[22] J. Marston and C. Zeng, J. Appl. Phys. **69**, 5962 (1991).
[23] N. Read and S. Sachdev, Nucl. Phys. B **316**, 609 (1989).
[24] O. Cepas, C. M. Fong, P. W. Leung, and C. Lhuillier, Phys. Rev. B **78**, 140405(R) (2008).
[25] M. Tovar, K. S. Raman, and K. Shtengel, Phys. Rev. B **79**, 024405 (2009).
[26] M. Hermele, Y. Ran, P. A. Lee, and X.-G. Wen, Phys. Rev. B **77**, 224413 (2008).
[27] S. Sachdev, Phys. Rev. B **45**, 12377 (1992).
[28] F. Wang and A. Vishwanath, Phys. Rev. B **74**, 174423 (2006).
[29] D. P. Arovas and A. Auerbach, Phys. Rev. B **38**, 316 (1988); A. Auerbach and D. P. Arovas, Phys. Rev. Lett. **61**, 617 (1988).
[30] S. Sachdev, arXiv:1002.3823 (unpublished).
[31] C. Xu and S. Sachdev, Phys. Rev. B **79**, 064405 (2009).
[32] L. Messio, O. Cépas, and C. Lhuillier, Phys. Rev. B **81**, 064428 (2010).
[33] J. Helton, K. Matan, M. Shores, E. Nytko, B. Bartlett, Y. Qiu, D. Nocera, and Y. Lee, Phys. Rev. Lett. **104**, 147201 (2010).
[34] M. Elhajal, B. Canals, and C. Lacroix, Phys. Rev. B **66**, 014422 (2002).
[35] A. Laeuchli and C. Lhuillier, arXiv:0901.1065 (unpublished).
[36] S. V. Isakov, T. Senthil, and Y.-B. Kim, Phys. Rev. B **72**, 174417 (2005).
[37] A. V. Chubukov, T. Senthil, and S. Sachdev, Phys. Rev. Lett. **72**, 2089 (1994); Nucl. Phys. B **426**, 601 (1994).
[38] M. Campostrini, M. Hasenbusch, A. Pelissetto, P. Rossi, and E. Vicari, Phys. Rev. B **63**, 214503 (2001).
[39] P. Calabrese, A. Pelissetto, and E. Vicari, Phys. Rev. E **65**, 046115 (2002).
[40] T. Grover and T. Senthil, arXiv:0910.1277 (unpublished).
[41] A. V. Chubukov, S. Sachdev, and J. Ye, Phys. Rev. B **49**, 11919 (1994).
[42] R. Singh, arXiv:1003.0138 (unpublished).